زانکۆی پۆلیتەکنیکی هەولێر
ERBIL POLYTECHNIC UNIVERSITY

Basim Mohammed Fadhil <basim.fadhil@epu.edu.iq>

[LAAR] Editor Decision

1 message

José L. Díaz de Tuesta via Open Journal Systems <laar.admin@plapiqui.edu.ar> 2 June 2023 at 12:11
Reply-To: "José L. Díaz de Tuesta" <joseluis.diaz@urjc.es>
To: "Dr. Niveen J. Abdulkader" <130012@uotchnology.edu.iq>, Payman Ahmed <payman.suhbat@koyauniversity.org>, "Ava A. K. Mohammed" <ava.mohammed@epu.edu.iq>, "Prof. Basim M. Fadhil" <basim.fadhil@epu.edu.iq>

Dear Dr. Niveen J. Abdulkader, Payman Ahmed, Ava A. K. Mohammed, Prof. Basim M. Fadhil:

We have reached a decision regarding your submission to Latin American Applied Research - An international journal, "REUSING MANUFACTURING WASTES AS CRACK RETARDANT".

We are pleased to inform that the work has been accepted and will be published in Latin American Applied Research.

Thank you very much for considering Latin American Applied Research journal,

Kind regards,

Subject editor

LAAR - Latin American Applied Research
http://laar.plapiqui.edu.ar/OJS/index.php/laar

Data Source

Wikipedia | Journal Homepage

Journal's Impact IF

2022-2023

0.702

↗ 281.5%

pact IF Trend

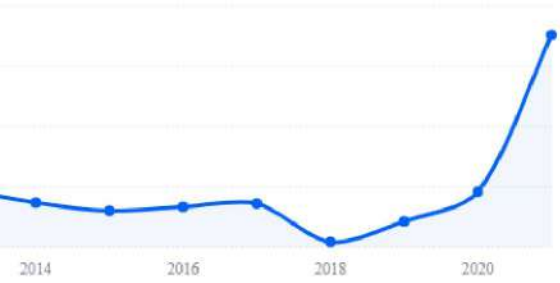

pact Ranking

LATIN AMERICAN APPLIED RESEARCH

Journal's Impact Ranking

	Quartile	Rank	Percentile
ing - General Chemical Engineering	-Q4	-241/280	-14%
al Chemistry	-Q4	-355/409	-13%
hanical Engineering	-Q4	-525/601	-12%

Top IF Gainers

eering - General Chemical Engineering	%
e Combustion Institute	+78.839%

REUSING COPPER ALLOY WASTES TO IMPROVE FRACTURE TOUGHNESS OF EPOXY

N.J. ABDULKADER†, P.S. AHMED‡, A.A.K. Mohammed†‡ and B.M. FADHIL‡‡

†*Department of Materials Engineering/University of Technology, Baghdad- Iraq*
‡*Manufacturing & Industrial Engineering Dept., Faculty of Engineering, Koya University, Koya KOY45, Kurdistan Region- F.R.Iraq*
Corresponding author, e-mail:payman.suhbat@koyauniversity.org,ORCID:https://orcid.org/0000-0003-3955-0512
†‡ *Department of Technical Mechanical and Energy Engineering, Erbil Technical Engineering College, Erbil Polytechnic University, Erbil, Iraq*
‡‡*Department of Automotive Technology, Erbil Technology College, Erbil Polytechnic University, Erbil, Iraq*

***Abstract*— In this work, a manufacturing waste is used as a reinforcement material for the epoxy to improve the fracture toughness, where the copper alloy machining chip is used with different weight fractions 5, 10, 15, and 20 wt. % and each percentage are added with three-chip lengths 0.6, 0.8, and 1.18 mm. Three-point bending test of the notched sample is used to test crack behaviour in addition to using materials characterization techniques to show the effect of the chip on structure, bonding, glass transition temperature (Tg), reinforcement dispersion, and fracture surface of the epoxy. Results show that adding the machining waste chips can enhance crack behaviour, and it is greatly dependent on the amount and size of the chip. The novelty of this research is in adding 20 wt.% - 0.8 mm length of copper alloy chips which improves the glass transition temperature and changes the fracture surface from brittle to ductile.**

***Keywords*— Machining chip, fracture toughness, stress intensity factor, composites materials.**

I. INTRODUCTION

The two main ways that society engages with the environment are as a provider of natural resources and as a repository for solid, gaseous, and liquid pollution (Fratila and Davim, 2013). People have become more consumerist as a result of population increase and technological advancements, which has had detrimental consequences on the environment such as mineral consumption, energy production, and waste production (Batista et al., 2021) Millions of metric tons of steel, coal, aluminum, and cobalt are used in global production. Recycling the waste from these metals can improve economic value while reducing environmental harm (Zhai and Yuan, 2012). As a result, numerous studies evaluated the reuse of metal chips in various applications, such as the use of steel chips as reinforcement in metal matrices (Yao et al., 2016) or the use of metal chips to sinter powder mixtures to create porous structures instead of using sand in the production of concrete (Alwaeli and Nadziakiewicz, 2012). (Alaneme and Odoni 2016, Gecu and Karaaslan, 2020). The strength of the densified product depends on the bonding between the matrix and the chips or between the chips and the chips. Consequently, how the chips interact with the matrix determines whether these applications are successful. For instance, concrete chips could oxidize (Batista et al., 2021). These enhancements made by researchers can be used to enhance Epoxy resin behavior.

Epoxy resins are a kind of high cross-link density thermoset polymers used in a variety of industries, such as adhesives, electronics, automotive, and aerospace. They function exceptionally well at high temperatures and have strong strength, high modulus, and little creep. Yet, the main problem when using Epoxy is that it loses its fracture toughness and brittleness due to its high cross-link density, rendering it prone to crack initiation and propagation (Bajpai et al., 2019).

By increasing fracture toughness and adding stiff fillers, such as carbon nano reinforcement (Bajpai et al., 2016), titanium oxide (Carballeira and Haupert, 2010), aluminum oxide (Wetzel, 2006), glass particles (Lee and Yee, 2000), and silicon oxide (Hsieh et al., (2010 a,b), Liang and Pearson, 2010), it is possible to increase the strength and modulus of epoxy without compromising the glass transition (Bajpai et al., 2019).

By using a simple maximum load failure criterion, material fracture toughness can be determined from load deflection curves seen during testing of notched flexural specimens (AL-Jeabory, 2001).

The main motivation of this research is to control the crack growth of Epoxy by adding copper alloy chips with various percentages and lengths which will act as an

obstacle against crack growth and retard crack propagation.

II. MATERIALS and METHODS

The utilization of production wastes to increase epoxy's stress intensity factor and fracture toughness is covered in this section.

A- Materials

Epoxy resin from Sika Company - Sikadur 52 base was used as a matrix, which is a low-viscosity liquid mixed with a hardener at a ratio of 2:1. Table 1 shows the matrix properties (Data sheet of Sikadur-52).

Table 1. properties of epoxy matrix (provided by the supplier).

Compression Strength	Flexural Strength	Tension Strength	Modulus of Elasticity
53 N/mm2	50 N/mm2	25 N/mm2	1.06 KN/mm2

The machining chip is collected and cleaned from dirt and grease, and then screened to obtain the three required sizes 0.6, 0.8- and 1.18-mm. Oxford X- Supreme 8000 XRF analyser was used to determine the chemical composition of the chip, as listed in Table 2.

Table 2. Chemical Composition of the chip.

Cu	Zn	Pb	Al	Sb	Si	Nb	S	Zr	Ni	Co	As
58.489	37.381	2.398	0.677	0.396	0.327	0.125	0.088	0.063	0.030	0.016	0.010

B- Methods

By adding machining chips with weight percentages of 5, 10, 15, and 20 wt.% as suggested by Nair (Nair et. Al., 2016) and Singha (Singha and Thakur, 2008), with three different chip lengths added for each percentage (0.6, 0.8, and 1.18 mm) as suggested by Abdullah et. Al. (Abdullah et. Al., 2017) to improve the mechanical properties, and comparing the results to pure epoxy as a reference (Table 3), the flexural test was used to assess the impact of manufacturing waste on the epoxy. The optimal lengths and chip-to-epoxy ratio are then determined. The impact of the chip on the epoxy's structure, bonding, glass transition temperature (Tg), dispersion, and fracture surface was demonstrated using Fourier transform infrared spectroscopy (FTIR), X-ray Fluorescence (XRF), Differential Scanning Calorimeter (DSC), and Field Emission Scanning Electron Microscope (FESEM).

The chip was added to the resin–hardener mix of the epoxy and then to the moulds made from acrylics by hand lay-up method, where the composite mixture was added from one corner into the mould to avoid bubble formation. Subsequently, the mixture was stored to be cured at room temperature for 7 days (Fadhil et al., 2016) The moulds were cut and prepared for the three-point bending test.

Table 3. Percentage and size of reinforcements used in this study.

Specimen No.	Reinforcement %	Size (mm)	Specimen No.	Reinforcement %	Size (mm)
1	0	---	8	15	1.18
2	5	1.18	9	15	0.6
3	5	0.6	10	15	0.8
4	5	0.8	11	20	1.18
5	10	1.18	12	20	0.6
6	10	0.6	13	20	0.8
7	10	0.8			

FTIR test is performed according to ASTM E1252, which is developed by Bruker Optics Company, Germany; its type is TENSOR-27. FTIR was used to examine and characterise the surface of the prepared composites ((ASTM E 1252-98, 2002). It is equipped with a room temperature DTGS detector, mid-IR source 4000–400 cm-1 and a KBr beam splitter.

DSC device (Perkin-Elmer Corporation), type (Shimadzu-DSC-60) is used to check if the chip addition reduces the glass transition temperature of Epoxy or improve its performance. Samples with a 10 mg mass were inserted in the holder along with a normal 40 µl aluminium crucible for the DSC test. As a reference holder, a different empty aluminium crucible of the same weight was 7 because a heater and a temperature sensor were included with each holder. The test was performed on samples, and each sample was heated at a range starting from −160 °C until 60 °C with a rate of 0 °C/min prior to cooling to room temperature.

FESEM-MIRA 3 LMU, MI 18112751Q was used to determine the chip dispersion and the behaviour of crack surface, whether it is brittle or improved, to show some ductility.

C-Fracture toughness test

A sample's resistance to fracture can be determined by fracture toughness. To gauge the fracture toughness of a sample put through the single-edge notched bending SENB test, the force applied to the movable center pin of the three-point bending test apparatus at the critical point should be measured. The critical point of a SENB test is defined as the maximum of the load-displacement curve, where an unstable fracture starts with increasing center pin displacement (Biswakarma et al., 2021). The fracture toughness, sometimes referred to as the critical stress intensity factor KIC, is computed using Eq. 1 (ASTM D5045-14, 2014), as follows (Bajpai and Wetzel, 2019):

$$K_{IC} = \frac{P}{BW^{0.5}} f\left(\frac{a}{W}\right) \quad (1)$$

where *P* is the applied load at the critical point, *B* is the thickness of material, *W* is the width of the material, and *a* is the length of the crack. The crack length is supposed to remain constant up until the point of unstable fracture for materials that follow linear elastic fracture mechanics (LEFM). According to the ASTM standard D5045-14 (ASTM D5045-14, 2014), the function *f* (a/W) is defined in Eq. 2 (Bajpai and Wetzel, 2019).

$$f\left(\frac{a}{w}\right) = f(\alpha) = \frac{(2+\alpha)}{(1-\alpha)^{3/2}} * (0.866 + 4.64\alpha - 13.32\alpha^2 + 14.72\alpha^3 - 5.6\alpha^4) \quad (2)$$

Fracture toughness or the energy release rate G_{IC} can be calculated using Eq. 3, as follows (Bajpai and Wetzel, 2019):

$$G_{IC} = \frac{K_{IC}^2(1-v^2)}{E} \quad (3)$$

where the *v* is the poison's ratio, which is set to 0.35, and *E* is the young's modulus in GPa (Bajpai and Wetzel, 2019).

According to ASTM D 5045 (ASTM D 5045-96, 1996), the three-point bending test was conducted to determine the material's fracture toughness and KIC using fractured specimens with dimensions of 100 mm in length, 80 mm in span length, 20 mm in width, and 5 mm in thickness (Fig. 1).

The crack front propagation on three-point bending specimens was investigated while taking the beginning notch length (a0=8.5 mm) into account. The notches were cut using a diamond sawing wire with a 0.28 mm semi-circular notch tip radius. The bending tests were conducted on a universal testing apparatus (Fig. 1) in the displacement control mode with a loading rate of 2.0 mm/min (Loya et al., 2010).

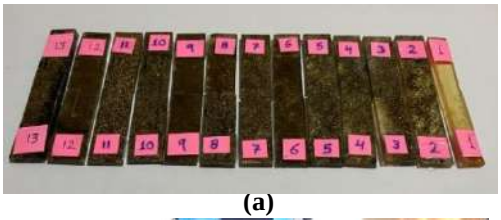

(a)

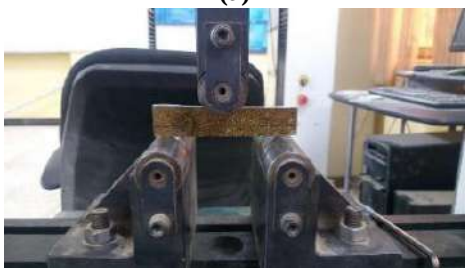

(b)

Figure 1: (a) notched 3-point bending samples, (b) universal bending test machine

III. RESULTS and DISCUSSION

This section explains the results and discussion of three-point bending test of notched in addition to DSC, FTIR, XRF and SEM test.

The FTIR curves of all composites are comparable to that of epoxy, indicating that no new phases were formed but the intensities of transmittance % were increased for almost all samples compared with that of epoxy which indicates a good physical bonding (Salih et al., 2018).

Fig. 2 shows the FTIR spectra of 5% reinforcementThe figure also shows that the intensity of the spectrum is increased compared with the epoxy spectrum because of the added chips.

The intensity of O-H stretching on the length of 0.6 mm is increased to less than 0.8 and 1.18 mm on 3400 cm^{-1}. Thus, the 0.6 mm length has less effect due to its shorter length because of the smaller bonding area between the chip and the Epoxy.

Moreover, the intensity of C-H stretching on 3000 cm^{-1} is increased for all added chips length. C=C stretching of the aromatic ring and N-H bending of primary amine on 1612 cm^{-1} are unaffected by any chip length.

A slight increase is found in the intensity of N-H bending of primary amine, C-C stretching of the aromatic ring, C-N stretching of imide, C-O-C stretching in ether linkage and C-H out of plane of the aromatic ring at 1570, 1512, 1384, 1035 and 750–572 cm^{-1}, respectively, in all chips lengths (Herrera et al., 2021).

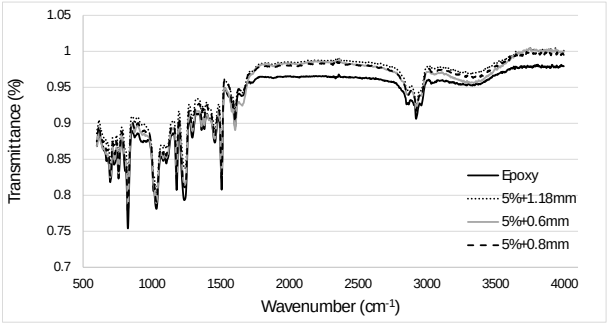

Figure 2: FTIR curves of 5% reinforced epoxy with 0.6, 0.8- and 1.18-mm length.

Figure 3 shows the FTIR spectra of 10% reinforcement. The figure shows that the intensity of O-H stretching and C-H stretching on the length of 1.18 mm is increased by more than 0.6 and 0.8 mm on 3400 and 3000 cm^{-1}, respectively, compared with epoxy resin due to its longer length because of the larger bonding area between the chip and the Epoxy. Thus, the 1.18 mm length has a higher effect. C=C stretching of the aromatic ring and N-H bending of the primary amine on 1612 cm^{-1} are unaffected by any chip length. A slight increase is found in the intensity of N-H bending of primary amine, C-C stretching of the aromatic ring, C-N stretching of imide, C-O-C stretching in ether linkage and C-H out of plane of the aromatic ring at 1570, 1512, 1384, 1035 and 750–572 cm^{-1}, respectively, in the 0.8 mm length. Moreover, a noticeble increase is achieved in the intensity of the

same bonds when adding 1.18 mm length because to its length and the increased surface where the chip and Epoxy are bonded, but adding 0.6 mm length does not affect the intensity of these bonds.

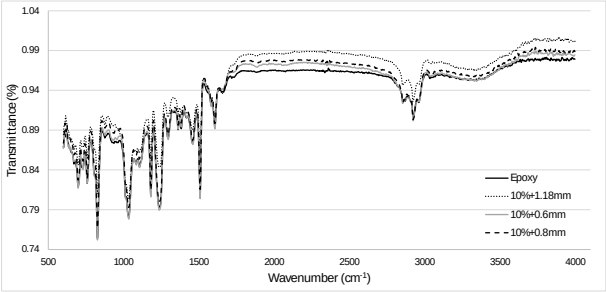

Figure 3: FTIR curves of 10% reinforced epoxy with 0.6, 0.8- and 1.18-mm length.

Figure 4 shows the FTIR spectra of 15% reinforcement. This figure shows that the intensity of O-H stretching on 3400 cm-1 is the same for 0.8 mm length as that of epoxy, but it is higher with the addition of 0.6 mm length, much higher with a shift in the bond when added by 1.18 mm length. Moreover, this bond widening and decrease indicates that some reactions, usually hydrogen bonding interaction, have occurred. In addition, the shift in the bond indicates a structural change. The C-H stretching on 3000 cm^{-1} for the lengths of 1.18 and 0.8 mm is the same as that of epoxy but it is higher when 0.6 mm length is added. A small increase in the intensity of C=C stretching of the aromatic ring and N-H bending of primary amine on 1612 cm^{-1} is found when adding 0.6 and 0.8 mm lengths. However, bond widening and shifting are obtained when adding 1.18 mm length, attributted to the increase in bond strength and structural change, as shown in the stress intensity factor results. On 1399 cm^{-1}, the intensity of C-N-C stretching of the imide ring and C-N stretching of imide on 1384 cm^{-1} are increased 0.8 and 1.18 mm length, but it is the same for 0.6 mm as pure epoxy. Under 1232 cm^{-1} C–O–C stretching of ether linkage, the intensities are increased for 0.6 and 1.18mm length but the same for 0.8 mm as pure epoxy. Under 1035 cm^{-1} C–O–C stretching of ether linkage and 828–800 cm^{-1} H–C= out-of-plane bending of MI ring and 1–4 substituted aromatic ring, the intensities are the same as those of epoxy for all lengths of chip reinforcement. Under 750–572 cm^{-1} C–H out-of-plane of aromatic ring the intensities are the same for 0.6- and 0.8-mm length, but it decreased to 1.18 mm when compared with pure epoxy because to its length and the increased surface where the chip and Epoxy are bonded.

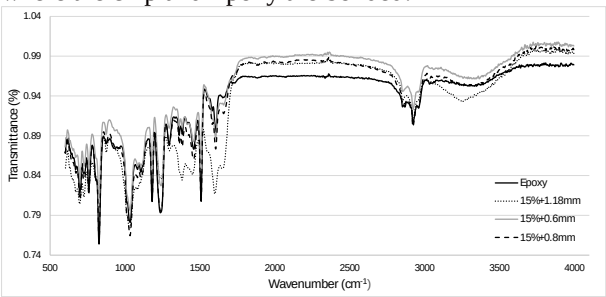

Figure 4: FTIR curves of 15% reinforced epoxy with 0.6, 0.8- and 1.18-mm length.

Figure 5 shows the FTIR spectra of 20% reinforcement. The figure shows that the intensity of O-H stretching on 3400 cm^{-1}, C-H stretching on 3000 cm^{-1}, C=C stretching of the aromatic ring and N-H bending of primary amine on 1612 cm^{-1}, N-H bending of primary amine with 1570 cm^{-1} length, C-C stretching of the aromatic ring on 1512 cm^{-1} and C-N stretching of imide on 1384 cm^{-1} increased with all lengths of the reinforcement chip. Under 1100 cm^{-1} of aromatic stretching, the intensity is the same when adding 0.6 mm length chip but it is increased when adding 0.8- and 1.18-mm length when compared with epoxy since it is longer and has a larger surface area where the chip and Epoxy are bonded. Under 1035 cm^{-1} C–O–C stretching of ether linkage, 828–800 cm^{-1} H–C= out-of-plane bending of MI ring and 1–4 substituted aromatic ring and 750-572 cm^{-1} C–H out-of-plane of aromatic ring, the intensities are the increased for all lengths of the chip reinforcement.

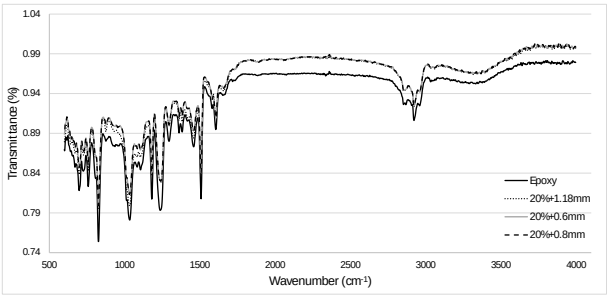

Figure 5: FTIR curves of 20% reinforced epoxy with 0.6, 0.8- and 1.18-mm length.

Figure 6 shows the stress intensity factor (KIC) results. The 5% and 10% reinforcements decrease the KIC of epoxy at all reinforcement lengths. This condition may be related to inhomogenity caused by these percentages (Fadhil et al., 2016) in the epoxy structure, which acts as stress raiser. However, the 15% reinforcement improves the stress intensity factor for all reinforcement lengths, where the KIC increased from 2.2 to 2.75, at 2.615 and 2.47 $MPa.m^{1/2}$ for 1.18, 0.8 and 0.6 mm reinforcements. This improvement is related to crack pinning (Domun et al, 2017), which occurs when the reifocement amount is sufficiently high to act as un obstacle against crack. Adding 20% leads to the highest improvement in KIC when the reinforcement is 0.6 mm in size. This finding is also related to the crack pining, where the KIC value increased to 2.75 $MPa.m^{1/2}$ as in the case of 15% with 1.18 mm length. However, using larger size of reinforcement to 0.8 and 1.18 mm leads to drawback in the KIC value due to inefficient dispersion and ineffectual cross-linking (Domun et al, 2017).

The effect of reinforcement size and percentages on the fracture toughness (G_{IC}) (Fig. 7) is close to their effect on the KIC except that in the case of sample no. 8 (15% with 1.18 mm length), where the G_{IC} is reduced. Different from KIC, this condition is due to the fact that the KIC is

dependent on the load, material dimension and design, as shown in equation 1, whereas the G_{IC} considers the material ductility and elongation in addition to the load and material design, as shown in Equation 2.

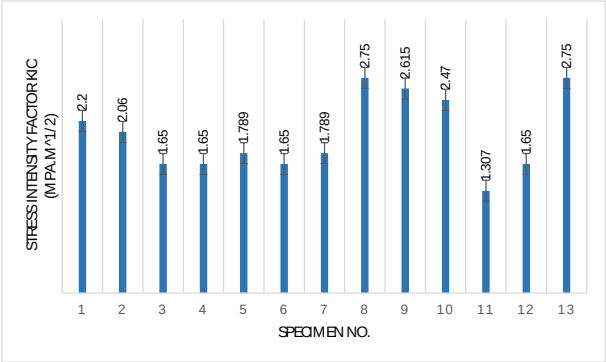

Figure 6: KIC values of chip reinforced epoxy composites used in this study.

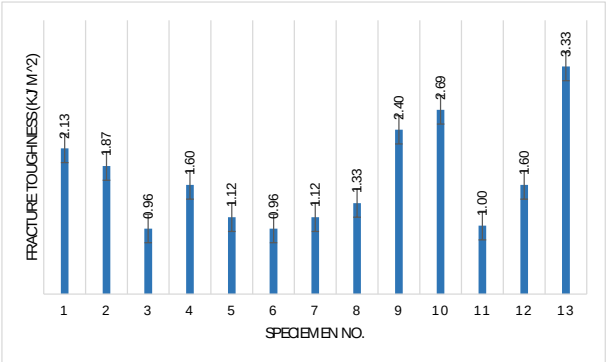

Figure 7: Fracture toughness (G_{IC}) values of chip reinforced epoxy composites used in this study.

Figure 8 shows the load extension curve of epoxy and samples no. 8 and 13. The figure shows that the extension of sample no. 8 (1.18 mm) is lower than that of epoxy (1.3 mm) and that of sample no. 13, despite the load of sample no. 8 (0.2 KN), is higher than that of epoxy (0.155 KN). This condition decreases the G_{IC} from 2.13 KJ/m^2 to 1.33 KJ/m^2, whereas the load (0.2 KN) and extension (1.6 mm) of sample no. 13 are higher than those of epoxy. Sample no. 13 is better that sample no. 8 because of its higher G_{IC}. The SEM images of the crack surface of epoxy and sample no. 13 are shown in Fig. 9. The change in crack behaviour from smooth and brittle for epoxy surface in the form of straight directions (which means when the crack intiated it will continue to grow fastly to fracture) Fig. 9. (a) to ductile and rough-containing bows (which means when crack intiated, it will need time to grow to fracture where the chip will act as an obsticle againt crack growth) Fig. 9. (b) for sample no. 13 surface is evident, indicating the increase in the G_{IC} of sample no. 13.

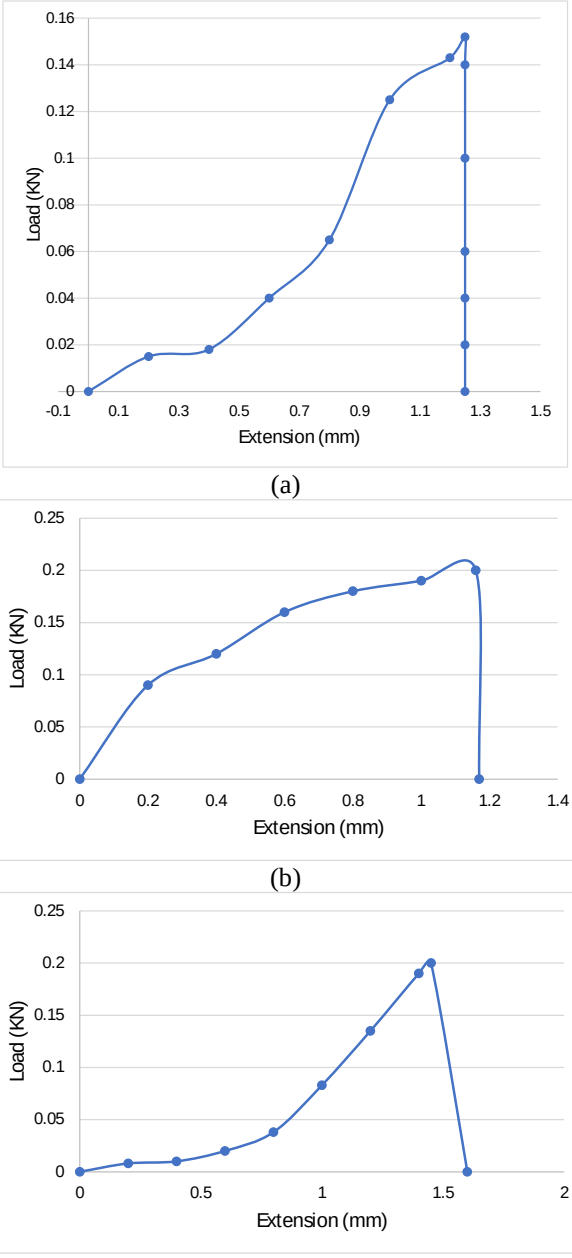

Figure 8: Load-extension curves of (a) Epoxy, (b) sample no. 8 and (c) sample no. 13.

The effect of adding 20 wt.% −0.8 mm length of chip on the glass transition temperature (Tg) of Epoxy is shown in Fig. 10. The figure shows that the addition of chip highly changed the glass transition temperature (Tg), where its value is increased from 150 ℃ to 200 ℃. The increase in Tg is most likely attributable to a decrease in the mobility of epoxy resin chain segments as a result of the Cu-Zn chip/matrix interactions (Lu et al., 2007) which is an another evident on increasing the strength.

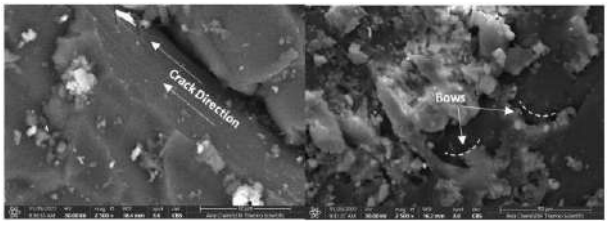

(a) (b)

Figure 9: SEM image of (a) epoxy at 2500x, (b) sample no.13 at 2500 x.

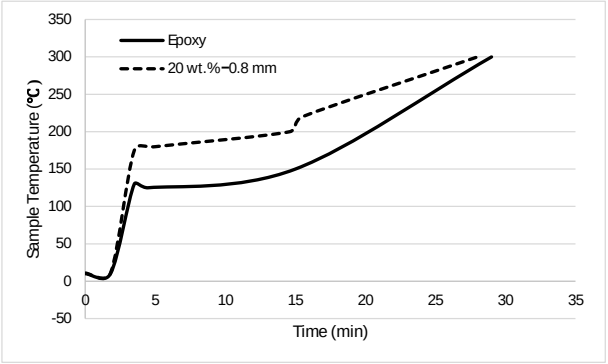

Figure 10: Glass transition temperature of epoxy resin and epoxy with 20 wt.% - 0.8 mm length of chip.

IV. CONCLUSIONS

In this work, a manufacturing waste is used as a reinforcement material for epoxy to improve the fracture toughness and the stress intensity factor. The machining chip is used with different weight fractions and three different lengths. The result shows that adding the machining wastes in the form of chips can enhance crack behaviour and the performance is greatly dependent on the amount and size of the chip. Moreover, adding 20 wt.% - 0.8 mm length of copper alloy chips which changes the glass transition temperature and change the fracture surface from brittle to ductile, thereby reducing the velocity of crack growth due to its good physical bonding and the larger bonding area between the chip and the Epoxy.

.

REFERENCES

1. Fratila, D., and Davim, J. P. (2013) *Green Manufacturing Processes and Systems, Materials Forming, Machining and Tribology*. Springer, Verlag Berlin Heidelberg.
2. Batista, C. D., Fernandes, A.A., Vieira, M. T. and Emadinia, O., (2021) From machining chips to raw material for powder metallurgy. *Materials.* **14**, 1-14.
3. Zhai, Q., and Yuan, Ch., (2012) Separation manufacturing metal chips for recycling through a combined hydrodynamic and electromagnetic approach. *In proceeding of 19th CIRP International Conference on Life Cycle Engineering*, Berkeley,167-168.
4. Alwaeli, M., Nadziakiewicz, J., (2012) Recycling of scale and steel chips waste as a partial replacement of sand in concrete. *Constr. Build. Mater.* **28**, 157-163.
5. Yao, B.B., Zhou, Z.Y., Duan, L.Y., Xiao, Z.Y., (2016) Compressibility of 304 stainless steel powder metallurgy materials reinforced with 304 short stainless-steel fiber. *Materials*, **9**, 1-11.
6. Alaneme, K.K., Odoni, B.U., (2016) Mechanical properties, wear and corrosion behavior of copper matrix composites reinforced with steel machining chip. *Int. J. Jestech*. **19**, 1593-1599.
7. Gecu, R., Karaaslan, A., (2020) Casting temperature dependent wear and corrosion behavior of 304 stainless steel reinforced A356 aluminium matrix bimetal composites fabricated by vacuum assisted melt infiltration. *Wear*, **446**.
8. Bajpai, A., Alapati, A. K., Klingler, A., and Wetzel, B., (2019) Effect of different types of block copolymers on morphology, mechanical properties, and fracture mechanisms of bisphenol-f based epoxy system. *J. Comp. Sci.*, **2**, 1-17.
9. Bajpai, A., Alapati, A. K., and Wetzel, B., (2016) Toughening and mechanical properties of epoxy modified with block co-polymers and MWCNTs. *Procedia Struct. Integr*, **2**, 104-111.
10. Carballeira, P., and Haupert, F., (2010) Toughening effects of titanium dioxide nanoparticles on TiO_2/ epoxy resin. *Polym. Compos.*, **31**.
11. Wetzel, B., Rosso, P., Haupert, F., Friedrich, K., (2006) Epoxy nanocomposites-fracture toughening mechanism. *Eng. Fract. Mech.*, **73**, 2375–2398.
12. Lee, J., and Yee, A.F., (2000) Fracture of glass bead/epoxy composites: On micro-mechanical deformations. *Polymer*, **41**, 8363–8373.
13. Hsieh, T.H., Kinloch, A.J., Masania, K., Taylor, A.C., (2010) The mechanisms and mechanics of the toughening of epoxy polymers modified with silica nanoparticles. *Polymer*, **51**, 6284–6294.
14. Liang, Y.L., Pearson, R.A., (2010) The toughening mechanism in hybrid epoxy-silica-rubber nanocomposites. *Polymer*, **51**, 4880–4890.

15. Hsieh, T.H., Kinloch, A.J., Masania, K., Lee, J.S., Taylor, A.C., (2010) The toughness of epoxy polymers and fibre composites modified with rubber microparticles and silica nanoparticles. *J. Mater. Sci.*, **45**, 1193–1210.
16. AL-Jeabory, J., (2001) The J- integral and KIc as a measure of fracture toughness of steel fibre concrete. *The Iraqi Journal for Mechanical and Material Engineering*, **Special Issue (C)**, 386-398.
17. ASTM D5045-14, Standard Test Methods for Plane-Strain Fracture Toughness and Strain Energy Release Rate of Plastic Materials; ASTM International: West Conshohocken, PA, USA, 2014.
18. Bajpai, A., and Wetzel, B., (2019) Effect of different types of block copolymers on morphology, mechanical properties, and fracture mechanisms of bisphenol-f based epoxy system. *J. Compos. Sci.*, **3**, 1-13.
19. Data sheet of technical properties of Sikadur-52 from Sika company.
20. Nair, J., J., Augustine, A., and Davanageri, M., B., (2016) Wear Characteristics and Vibration Analysis of Shell Powder Filled Glass Fiber Reinforced Epoxy Composite Laminates, *Int. J. Eng. Res. Technol*, **5**, 215–21
21. Singha, A., S., and Thakur, V., K., (2008) Mechanical properties of natural fibre reinforced polymer composites, *Bull. Mater. Sci.*, **31**, 791–9.
22. Abdullah, S., A., Hamad, G., G., (2017) Study the effect of adding low weight percentage of Brass chips on the mechanical properties of Epoxy, *graduation project*, Erbil Polytechnic University, Kurdistan region, Iraq.
23. Fadhil, B., Ahmed, P., and Kamal, A., (2016) Improving mechanical properties of epoxy by adding multi-wall carbon nanotube. *J. of Theo. and App. Mech*. **54**, 551-560.
24. Biswakarma, J. S., Cruz, D. A., Bain, E. D., Dennis, J. M., Andzelm, J.W., and Lustig, S. R., (2021) Modeling brittle fractures in epoxy nanocomposites using extended finite element and cohesive zone surface methods. polymers, **13**, 1-13.
25. ASTM E 1252-98, Annual Book of ASTM Standard, 2002. Standard Practice for General techniques for Obtaining Infrared Spectra for Qualitative Analysis, E 1252-98, pp. 1-11.
26. ASTM D 5045–96, Standard Test Method for Plane-Strain Fracture Toughness and Strain Energy Release Rate of Plastic Materials. American Society for Tensting and Materials, Philadelphia, 1996.
27. Loya, J.A., Villa, E.I., Fernandez-Saez, J. (2010) Crack-front propagation during three-point-bending tests of polymethyl-methacrylate beams. *Polym. Test.* **29**, 1, 113-118.
28. Salih, S. I., Oleiwi, J. K., Ali, H. M., (2018) Study the Mechanical Properties of Polymeric Blends (SR/PMMA) Using for Maxillofacial Prosthesis Application. *IOP Conf. Ser.*: Mater. Sci. Eng. 454 012086.
29. Herrera, C. A., Cruz, I. C. and Cedeno, I. H. Romero, O. M. and Zuniga, A. E. (2021) Influence of Epoxy resin process parameters on the mechanical properties of produced bidirectional [45^{o}] carbon/Epoxy woven composites. *Polymers*, **13**, 1-12.
30. Domun, N., Hadavinia, H., Zhang, T., Liaghat, Gh., Vahid, S., Spacie, Ch., Paton, K. R., and Sainsbury, T., (2017) Improving the fracture toughness properties of epoxy using graphene nanoplatelets at low filler content. *Nanocomposites*, **3**, 85-96.
31. Lu, Sh., Wei, Ch., Yu, J., Yang, X. and Jiang, Y. (2007) Preparation and characterization of epoxy nanocomposites by using PEO-grafted silica particles as modifier. *J Mater Sci*, **42**, 6708–6715.